

Dynamic Power and Energy Capabilities of Commercially-Available Electro-Active Induced-Strain Actuators

VICTOR GIURGIUTIU* AND CRAIG A. ROGERS

Center for Intelligent Material Systems and Structures, Virginia Polytechnic Institute and State University, Blacksburg, VA 24061-0261

ABSTRACT: A method has been developed to predict the apparent material constants, the input and output power and energy, and the electro-mechanical energy conversion efficiency of electro-active induced-strain actuators under full-stroke, quasi-linear dynamic operation. The effect of the piezo-electric counter electro-motive force on the apparent input admittance is included. The non-symmetric expansion-retraction behavior of the electro-active material under full-stroke dynamic operation is symmetrized using a bias-voltage component and a superposed dynamic voltage amplitude that produce, in the actuator, a static position and a dynamic stroke amplitude, respectively. It is shown that the presence of the bias-voltage operation increases significantly the reactive power amplitude, and a simple formula for estimating this increase is provided. Reaction power values up to three times larger than those for unbiased operation were found.

The secant linearization method and vendor data were used to evaluate the full-stroke piezo-electric strain coefficient, d , elastic compliance, s , electrical permittivity, ϵ , and electro-mechanical coupling coefficient, κ , of the electro-active actuator. Consistency with the basic active-material values was checked, and correction of the actuator full-stroke electro-mechanical coupling coefficient was applied, when required. Maximum power and energy delivery under optimal dynamic conditions (dynamic stiffness match) was studied, and the dynamic energy output capability of several commercially-available actuators were computed. Output energy densities per unit volume, mass, and cost were also calculated. The best electro-mechanical conversion efficiency, which was shown to take place at stiffness ratios slightly different from the dynamic stiffness match, was also computed.

INTRODUCTION

THE development of solid-state induced-strain actuators (ISA) has entered the production stage, and actual actuation devices based on these concepts are likely to reach the applications market in the next few years. An increasing number of vendors are producing and marketing solid-state actuation devices based on induced-strain principles. However, the performance of the basic induced-strain actuation materials used in these devices, and the design solutions used in their construction, are found to vary from vendor to vendor. This variability aspect presents a difficulty for the design engineer who intends to utilize the solid-state induced-strain actuators as prime movers and needs a uniform set of design information.

Recognizing this need, the Center for Intelligent Material Systems and Structures at Virginia Tech has initiated an induced-strain actuators database using vendor information and a set of energy-based performance metrics such as: maximum output energy; energy densities per unit mass, volume, and cost; energy conversion efficiency; etc. The first task in this work was to compute and compare the performance of induced-strain actuators under static regime (Giurgiutiu, Rogers, and Chaudhry, 1996). In a con-

tinuation effort, the present study presents the performance of induced-strain actuators under dynamic regime. Since the behavior of induced-strain actuators under expansion and contraction regimes is strongly non-symmetrical, the dynamic performance cannot be directly extrapolated from the static results. This paper shows how the bias position and the dynamic displacements are computed from vendor data, and points out that the presence of bias voltage can increase the actuator reactive power requirements by up to three times. In addition, the theoretical approach taken in the present paper is much more detailed than that of Giurgiutiu, Rogers, and Chaudhry (1996) since it uses a complete dynamic model for the external load (mass, stiffness, damping), accounts for the dynamic losses in the stack through complex stiffness and complex permittivity representation, and includes the piezo-electric counter electro-motive force effect on the apparent input capacitance of the actuator. The study derives prediction formulae for the effective full-stroke electromechanical coupling coefficient of the actuator, and for the power and energy conversion efficiency. The maximum output energy and the best conversion efficiency under dynamic conditions are derived. It is shown that the dynamic stiffness ratio match condition ensures maximum output energy, but does not ensure best conversion efficiency, which happens at a slightly higher stiffness ratio value.

*Author to whom correspondence should be addressed.

The present study addresses only electro-active induced-strain actuators, based on the linear theory of piezo-electricity. A further study, based on the linear theory of piezo-magnetism, which covers the magneto-active induced-strain actuators, is underway and will be presented at a later stage.

THEORETICAL BACKGROUND

Basic Equations of Linear Electro-Active Material Behavior

The general constitutive equations of linear electro-active material behavior, given by ANSI/IEEE Standard 176-1987, describe a tensorial relation between mechanical and electrical variables (mechanical strain S_{ij} , mechanical stress T_{ij} , electrical field E_i , and electrical displacement D_i) in the form:

$$\begin{aligned} S_{ij} &= s_{ijkl}^E T_{kl} + d_{kij} E_k \\ D_j &= d_{jki} T_{kl} + \epsilon_{jk}^T E_k \end{aligned} \quad (1)$$

where s_{ijkl}^E is the mechanical compliance of the material measured at zero electric field ($E = 0$), ϵ_{jk}^T is the dielectric permittivity measured at zero mechanical stress ($T = 0$), and d_{kij} is the piezo-electric coupling between the electrical and mechanical variables. The second equation reflects the *direct piezo-electric effect*, while the first equation refers to the *converse piezo-electric effect*.

Typical electro-active induced-strain actuators are stacks of thin active-material layers, alternatingly charged (Figure 1). In such an electro-active material stack, mechanical stress and electric field act only in the 3-direction (the stack axis), and the transverse effects can be neglected in a first-order analysis. The one-dimensional equivalent of Equation (1) is, simply,

$$\begin{aligned} S &= s \cdot T + d \cdot E \\ D &= d \cdot T + \epsilon \cdot E \end{aligned} \quad (2)$$

where the subscripts "3", "33", "333", and "3333" are implied, as appropriate. The compliance, s , is assumed to be measured at zero electric field, while the permittivity, ϵ , is measured at zero stress.

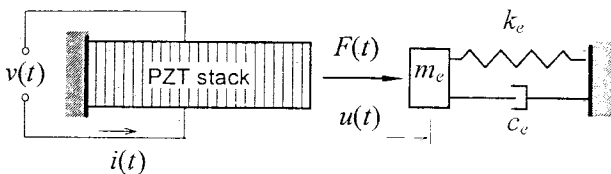


Figure 1. Schematic representation of a solid-state induced-strain actuator (PZT stack) operating against a mechanical load.

Electro-Mechanical Description of an Induced-Strain Actuator Operating a Mechanical Load

Most commercially-available induced-strain actuators are rated for voltage and displacement values that ensure quasi-linear behavior. This allows the use of a linear electro-mechanical model in the analysis. Giurgiutiu, Chaudhry, and Rogers (1994) gave a dynamic-stiffness representation of a solid-state induced-strain actuator (PZT stack) operating a mechanical load of parameters k_e , m_e , and c_e (Figure 1). The PZT stack is energized by a voltage source, $v(t)$, which sends a current, $i(t)$, that builds up the internal charge. As the charge is built up, the voltage and the electric field increase. Under the action of the electric field, the electro-active material expands and produces an output displacement, $u(t)$, which generates a reaction force from the mechanical system, $F(t)$. The reaction force, $F(t)$, acting on the PZT stack, induces loss of output displacement through the stack compressibility and through the counter electric motive force (emf) due to the piezo-electric effect. Hence, an actuator under load always has a lower output displacement than a load-free actuator energized by the same voltage. A detailed analysis of the configuration shown in Figure 1, starting from the basic electro-mechanical constitutive equations of active material behavior and using wave propagation techniques, was given by Giurgiutiu, Chaudhry and Rogers (1994). For operation frequencies below 100 Hz, the wave propagation effects can be ignored, and the equivalent input admittance was found to be:

$$Y(\omega) = i\omega C \left(1 - \frac{d^2}{s\bar{\epsilon}} \frac{\bar{r}(\omega)}{1 + \bar{r}(\omega)} \right) \quad (3)$$

where C is the zero-load capacitance of the stack, d is the zero-load induced-strain coefficient, \bar{s} is the open-circuit (zero-field) complex mechanical compliance of the stack, and $\bar{\epsilon}$ is the zero-load complex electrical permittivity (dielectric constant) of the active material, i.e.,

$$\bar{s} = s(1 - i\eta) \quad (4)$$

$$\bar{\epsilon} = \epsilon(1 - i\delta) \quad (5)$$

with η being the hysteresis internal damping coefficient, and δ the dielectric loss coefficient. The coefficient $\bar{r}(\omega)$ is the complex stiffness ratio:

$$\bar{r}(\omega) = \bar{k}_e(\omega)/\bar{k}_i \quad (6)$$

where the complex stiffness expressions are:

$$\bar{k}_i = \frac{A}{s l} \quad (\text{complex internal stiffness}) \quad (7a)$$

$$\begin{aligned} \bar{k}_e(\omega) &= (k_e - \omega^2 m_e) + i\omega c_e \\ &(\text{complex external stiffness}) \end{aligned} \quad (7b)$$

The Apparent Electro-Mechanical Constants of an Existing Induced-Strain Actuator

One can define apparent electro-mechanical constants of an electro-active induced-strain actuator using the overall performance data available in the vendor catalogues. In doing this, one is effectively using the secant method to linearize the full-stroke behavior of the actuator. Hence, apparent values of the piezo-electric strain coefficient, d , elastic compliance, s , electrical permittivity, ϵ , and electro-mechanical coupling coefficient, κ , can be calculated. By definition:

$$\hat{u}_{ISA} = l \frac{V}{t} d \quad (\text{dynamic free stroke}) \quad (8a)$$

$$C = \frac{\epsilon A}{t} N_{layers} = \frac{\epsilon A l}{t} \quad (\text{stress-free capacitance}) \quad (8b)$$

$$k_t = \frac{A}{ls} \quad (\text{actuator stiffness}) \quad (8c)$$

where l is the stack length, t is the layer thickness, and A is the stack cross-sectional area. Hence:

$$d = \frac{\hat{u}_{ISA} t}{V l} \quad (\text{apparent piezo-electric strain coefficient}) \quad (9a)$$

$$\epsilon = \frac{C t^2}{A l} \quad (\text{apparent zero-stress electrical permittivity}) \quad (9b)$$

$$s = \frac{A}{lk_t} \quad (\text{apparent zero-field elastic compliance}) \quad (9c)$$

According to the IEEE Standard on Piezo-electricity (ANSI/IEEE Std 176-1987), the electro-mechanical coupling coefficient, relevant to the 33-direction in which the induced-strain actuator operates, is:

$$(k'_{33})^2 = \frac{d_{33}^2}{s_{33}^E \epsilon_{33}^T} \quad (10)$$

Consistent with the linearization scheme, the constants d_{33} , ϵ_{33}^T , s_{33}^E , are given by Equations (9a)–(9c). Denoting k'_{33} by κ (to avoid confusion with the notation, k , already used for the mechanical stiffness) we arrive at the following simple expression for the full-stroke electro-mechanical coupling coefficient of the actuator:

$$\kappa^2 = \frac{k_t \hat{u}_{ISA}^2}{CV^2} \quad (11)$$

Equation (11) can be easily recognized as the ratio between the reference mechanical energy, $\hat{E}_{mechanical} = (1/2)$

$k_t \hat{u}_{ISA}^2$, and the reference electrical energy, $\hat{E}_{electrical} = (1/2) CV^2$. The simplicity of Equation (11) is remarkable. Equation (11) can be used for a rapid consistency check on the vendor data for a given electro-active induced-strain actuator. Table 1 presents values of the full-stroke electro-mechanical coupling coefficient, κ , for fourteen commercially-available actuators derived with Equation (11) from vendor data. Examination of the κ values given in Table 1 reveals that, in some cases, values close to 1.0 appear. However, the electro-mechanical coupling coefficient of the basic electro-active material is known not to exceed the value 0.75. This apparent inconsistency may stem from the fact that the mechanical stiffness and the electric capacitance provided by vendors are usually derived from small-amplitude tests, while, for large-amplitudes, a non-linear variation may be present. Since non-linear values are not included in the vendor data, a correction procedure had to be applied, and the full-stroke electro-mechanical coupling coefficient of the active-material stack was limited to the upper bound value of 0.75. The corrected electro-mechanical coupling coefficient is given as κ' in Table 1.

The electro-mechanical coupling coefficient can be effectively used to simplify the electro-mechanically coupled expression of the complex admittance given by Equation (3). Upon substitution of

$$\frac{d^2}{s\epsilon} = \kappa^2 \quad (12)$$

Equation (3) becomes:

$$Y(\omega) = i\omega C \left(1 - \kappa^2 \frac{\bar{r}(\omega)}{1 + \bar{r}(\omega)} \right) \quad (13)$$

Electrical Power with Bias Voltage

Electro-active solid-state induced-strain actuators do not have a symmetrical behavior when the polarity of the applied voltage is reversed under full-stroke operation. A preferred polarity exists which generates the maximum expansion. Under reversed polarity, some limited contraction may be achieved. Hence, dynamic operation must take place about a mid-range position, which is achieved by superposing a bias component onto the dynamic component. For biased operation, the applied voltage has the general expression:

$$v(t) = V_0 + V \sin \omega t \quad (14)$$

where V_0 is the bias voltage, and V is the dynamic voltage amplitude. The corresponding induced-strain displacement has the expression:

$$u_{ISA}(t) = u_0 + \hat{u}_{ISA} \sin \omega t \quad (15)$$

where, u_0 is the bias position, and \hat{u}_{ISA} is the dynamic dis-

Table 1. Vendor data and calculated results for 14 commercially-available induced-strain actuators used in dynamic applications.

Identification	Active Material Type	Stiffness k_f (kN/mm)	Electrical Capacitance C (μ F)	Max. Free Expansion u_{ISA}^+ (μ m)	Max. Free Contraction u_{ISA}^- (μ m)	Expansion Voltage V^+ (V)	Contraction Voltage V^- (V)
Polytec PI							
P-245.70	HVPZT	8.0	0.45	120	-30.0	-1000	250
P-246.70	HVPZT	190.0	3.00	120	-30.0	-1000	250
P-247.70	HVPZT	370.0	5.60	120	-30.0	-1000	250
P-844.60	LVPZT	33.0	43.00	90	-22.5	-100	25
EDO Corp.							
E100P-2	PMN	100.0	0.06	18	0.0	800	0
E300P-4	PMN	160.0	1.60	66	0.0	800	0
E400P-3	PMN	220.0	0.58	40	0.0	800	0
Burleigh Instruments							
PZL-060	PZT	3.9	3.10	60	-16.0	150	-40
AVX Corp. (AVX-PMN Young's modulus was taken 91 GPa, and AVX-PZT modulus was taken 70 GPa)							
AVX-PMN	PMN	125.6	4.50	17.5	0.0	150	0
AVX-PZT	PZT	126.3	4.50	13.5	-3.6	150	-40
TOKIN							
LA-10 \times 10 \times 1	PZT	228.9	6.50	15	0.0	100	0
Morgan Matroc Inc.							
70044-1	PZT-5H	1080.0	2.50	9.75	0.0	250	0
70050-1	PZT-5H	1280.0	11.40	15.01	0.0	250	0
70051-1	PZT-5H	2000.0	12.40	15.01	0.0	250	0

placement amplitude. The values \hat{V}_0 , V , u_0 and \hat{u}_{ISA} are easily calculated from manufacturers' specifications. For example (Figure 2), the solid-state induced-strain actuator P-247.70 produced by Polytec PI, Inc., obtains its maximum free expansion of 120 μ m under a voltage of -1000 V, and

has a maximum contraction of -30 μ m under a voltage of 250 V. For this actuator, the applied voltage for most productive dynamic operation will be $v(t) = (-375) + (-625) \sin \omega t$ V, with $V_0 = [(-1000) - (-250)]/2 = -375$ V and $V = [(-1000) + (-250)]/2 = -625$ V.

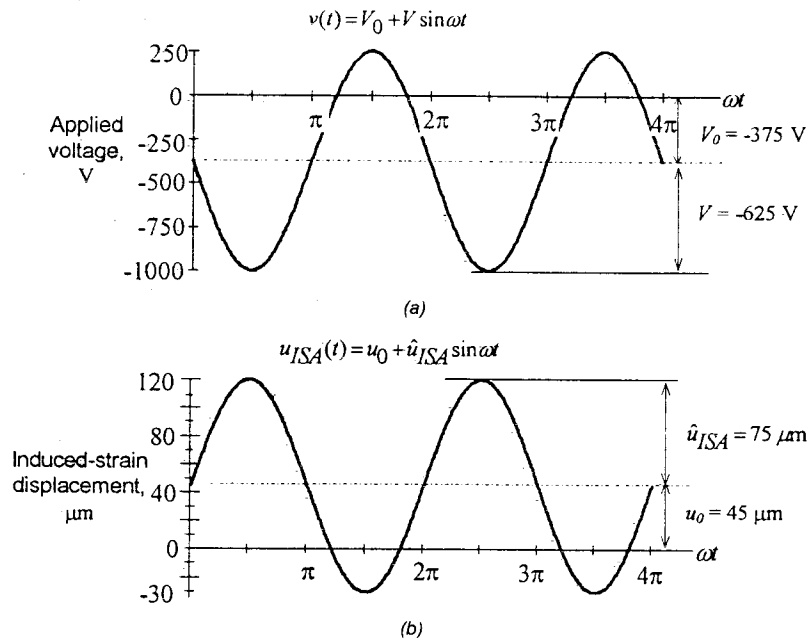


Figure 2. Dynamic operation of Polytec PI P-247.70 induced-strain actuator: (a) applied voltage, $v(t)$, has bias and dynamic components, V_0 and V and (b) the corresponding induced-strain displacement, $u_{ISA}(t)$.

The resulting dynamic displacement is $u_{ISA}(t) = 45 + 75 \sin \omega t \mu\text{m}$, with $u_0 = (120 - 30)/2 = 45 \mu\text{m}$ and $\hat{u}_{ISA} = (120 + 30)/2 = 75 \mu\text{m}$. Other solid-state induced-strain actuators have no reversed polarity operation, like, for example, the actuator E300P-4 produced by EDO Corporation. This actuator attains its maximum expansion at 800 V, but accepts no voltage reversal. For E300P-4, the excitation voltage for dynamic operation will be $v(t) = 400 + 400 \sin \omega t \text{ V}$, with $V_0 = V = 800/2 = 400 \text{ V}$, whereas the resulting displacement is $u_{ISA}(t) = 30 + 30 \sin \omega t \mu\text{m}$ with $u_0 = \hat{u}_{ISA} = 30 \mu\text{m}$.

The power requirements of an induced-strain actuator operating with bias voltage are calculated using the equivalent electric circuit having the general expression for the complex electric admittance, i.e.,

$$\bar{Y} = \left[R + i \left(\omega L - \frac{1}{\omega C} \right) \right]^{-1} \quad (16)$$

Writing the electric current as:

$$i(t) = I \sin(\omega t - \phi), \quad \phi = \tan^{-1} \left[\left(\omega L - \frac{1}{\omega C} \right) / R \right] \quad (17)$$

one calculates the electric current amplitude, I , as:

$$I = Y(\omega)V \quad (18)$$

By definition, *electrical power = voltage × current*, and hence,

$$P(t) = v(t) \cdot i(t) = (V_0 + V \sin \omega t) \cdot I \sin(\omega t - \phi) \quad (19)$$

Expansion of Equation (19) gives:

$$P(t) = \frac{1}{2} VI \cos \phi - \frac{1}{2} VI \cos(2\omega t - \phi) + V_0 I \sin(\omega t - \phi) = P_{active} + P_{reactive}(t) \quad (20)$$

Note that the active component of power is not influenced by the bias voltage and has the expression $P_{active} = (1/2) VI \cos \phi$, while the reactive component of power has the modified expression:

$$P_{reactive}(t) = -\frac{1}{2} VI \cos(2\omega t - \phi) + V_0 I \sin(\omega t - \phi) \quad (21)$$

The influence of the bias voltage, V_0 , is to increase significantly the reactive power component. The complex power amplitude, $|\bar{P}| = (1/2) VI$, can be factored out of Equation (20), and hence,

$$P_{reactive}(t) = |\bar{P}| (-\cos(2\omega t - \phi) + 2v_0 \sin(\omega t - \phi)) \quad (22)$$

where,

$$v_0 = V_0/V \quad (23)$$

is the *bias voltage coefficient*. Electro-active induced-strain actuators are mainly capacitive, and their phase angle is close to -90° . For $\phi = -90^\circ$, Equation (22) becomes:

$$P_{reactive}(t) = |\bar{P}| (\sin(2\omega t) + 2v_0 \cos(\omega t)) \quad (24)$$

Figure 3 presents the time-variation of the normalized reactive power for various values of the bias voltage coefficient, v_0 . Note that, for $-1 < v_0 < 1$, the reactive power curve shows a pair of local maxima, of which only one is also global maximum, i.e., the peak value of the reactive power per cycle. For $v_0 = 1$, the curve has a horizontal-tangent inflection point at $3\pi/2$. For $v_0 > 1$ and for $v_0 < -1$, the reactive power curve presents only one maximum since its behavior is dominated by the bias-voltage component. For ϕ slightly different from 90° , curves similar to those given in Figure 3 are obtained.

To calculate the peak value per cycle of the reactive power, one can differentiate Equation (24) with respect to ωt and set the derivative to zero. The resulting quadratic equation has a pair of solutions of which only one corresponds to the peak reactive power. Thus, the peak reactive power takes place at the following critical angular values:

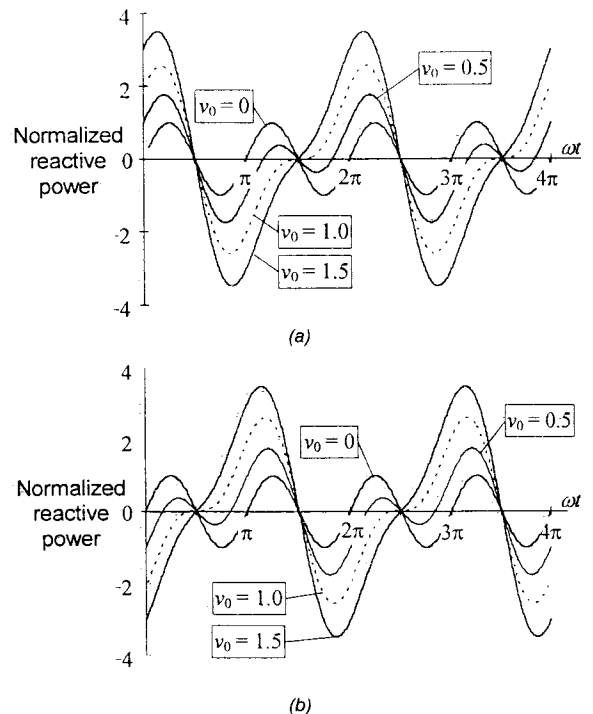


Figure 3. Variation of normalized reactive power for $\phi = -90^\circ$: (a) positive bias coefficient and (b) negative bias coefficient.

$$(\omega t)_{cr} = \sin^{-1} \left(-\frac{v_0}{4} + \frac{1}{4}\sqrt{v_0^2 + 8} \right), \quad \text{for } v_0 > 0 \quad (25)$$

$$(\omega t)_{cr} = \sin^{-1} \left(-\frac{v_0}{4} - \frac{1}{4}\sqrt{v_0^2 + 8} \right), \quad \text{for } v_0 > 0 \quad (26)$$

The variation of the critical angular values, ωt_{cr} , with the bias voltage coefficient is shown in Figure 4. The value of ωt_{cr} decreases as the bias voltage coefficient, v_0 , increases [Figure 4(a)]. The normalized peak reactive power varies with v_0 , as shown in Figure 4(b). Using Figure 4(b), one can define a reactive power correction coefficient, $\chi(v_0)$, which accounts for the increase in the peak reactive power due to the bias voltage operation. Thus,

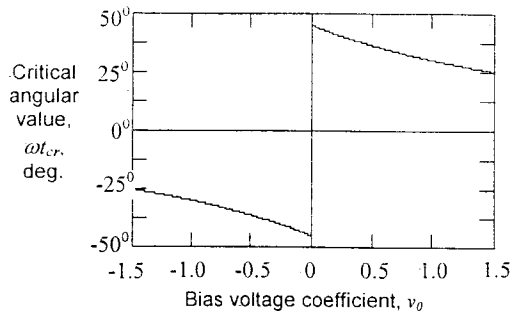
$$P_{reactive}^{peak} = \chi(v_0) |\bar{P}| \quad (27)$$

For a limited range of v_0 , the curve shown in Figure 4(b) is almost linear, though its algebraic expression (not given here for brevity) is quite elaborate. A reasonable approximation for the reactive power correction coefficient in the range $-1.5 < v_0 < 1.5$ is given by the formula:

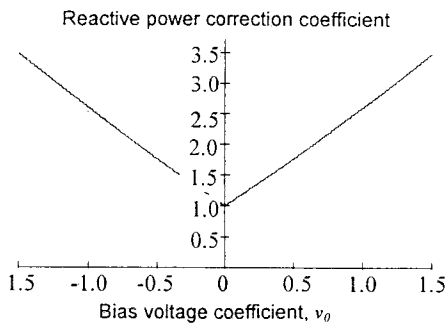
$$\chi(v_0) \approx 1 + 1.62 |v_0| \quad (28)$$

Electrical Power Input to an Induced-Strain Actuator

Assume biased operation with input voltage, $v(t) = V_0 + V \sin \omega t$, where the voltage amplitude, V , and bias



(a)



(b)

Figure 4. Influence of the bias voltage coefficient on the reactive power: (a) variation of the critical angular values, ωt_{cr} and (b) reactive power correction coefficient.

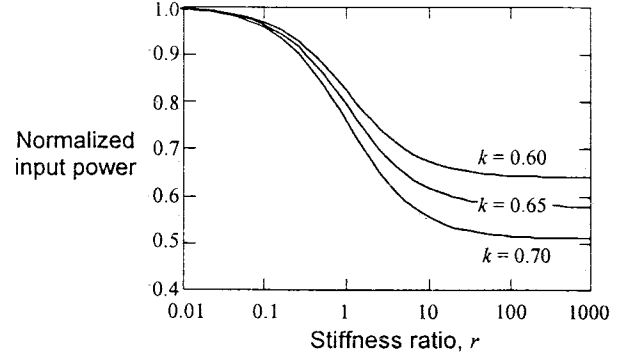


Figure 5. Variation of input power with stiffness ratio for three values of the electromechanical coupling coefficient, κ .

voltage, V_0 , are chosen in such a way as to obtain maximum dynamic displacement of the actuator. Using Equations (27) and (28), we express the peak reactive power per cycle as:

$$P_{reactive}^{peak} = \chi(v_0) |\bar{P}_{electr}| \quad (29)$$

where $\bar{P}_{electr} = (1/2) \bar{Y} V^2$ is the complex electrical power. Upon substitution of Equation (13) into Equation (29), we get the following expression for the peak input power per cycle of an electro-active induced-strain actuator:

$$P_{in} = \frac{1}{2} \chi(v_0) \left| i\omega C \left(1 - \kappa^2 \frac{\bar{r}(\omega)}{1 + \bar{r}(\omega)} \right) \right| V^2 \quad (30)$$

The power input varies with the frequency-dependent complex stiffness, $\bar{r}(\omega)$. For a low-damping mechanical system, driven well below the mechanical resonance frequency, the complex stiffness ratio is predominantly real, i.e., $\bar{r} \approx r$. Thus, the peak value per cycle of the electrical power input takes the simpler form:

$$P_{in} = \omega \cdot \chi(v_0) \left(1 - \kappa^2 \frac{r}{1+r} \right) \left(\frac{1}{2} C V^2 \right) \quad (31)$$

The last factor in Equation (31) represents the reference electrical energy amplitude, $(1/2) C V^2$, that can be easily calculated, for a given active-material stack, from manufacturers' specifications. The first factor in Equation (31) shows that the input power increases linearly with frequency, as expected for a predominantly reactive electrical load. The second and third factors in Equation (31) are modifiers that take into account the bias voltage effects and the external loading conditions, respectively. Equation (31) shows that, at a given frequency, the peak input power per cycle varies strongly with the stiffness ratio, r . Figure 5 gives a plot of the normalized peak input power vs. stiffness ratio, r . It is apparent that the peak input power per cycle decreases as the stiffness ratio increases. For a fully-blocked actuator ($r \rightarrow \infty$), the relative reduction in peak input power is maximum, and equal to κ^2 . Practical values of κ vary between 0.6 and 0.7, with a potential power reduction of as much as

50% for a fully blocked actuator. However, this reduction may not be of great practical significance since a fully blocked actuator has zero output displacement and hence does not deliver any power output. Further discussion of these effects can be found in the subsequent section dealing with electro-mechanical power conversion efficiency.

Mechanical Power Output from an Induced-Strain Actuator

By definition, *mechanical power* = *force* × *velocity*. For harmonic motion, the expression of the complex power is $\bar{P} = (1/2)\bar{F} \cdot \bar{v}^*$, where \bar{v}^* is the complex conjugate of \bar{v} , and $\bar{v} = i\omega\bar{u}$. Using the output displacement amplitude

$$\bar{u} = \frac{1}{1 + \bar{r}(\omega)} \hat{u}_{ISA} \quad (32)$$

with \hat{u}_{ISA} given by Equation (8a), we write the output mechanical power as:

$$\bar{P}_{out} = \frac{1}{2} \bar{k}_e \bar{u} (i\omega \bar{u})^* = \frac{1}{2} \bar{k}_e \frac{1}{1 + \bar{r}(\omega)} \left(\frac{i\omega}{1 + \bar{r}(\omega)} \right)^* \hat{u}_{ISA}^2 \quad (33)$$

Upon simplification,

$$\bar{P}_{out} = -i\omega \frac{\bar{r}(\omega)}{(1 + \bar{r}(\omega))(1 + \bar{r}(\omega))^*} \left[\frac{1}{2} k_i \hat{u}_{ISA}^2 \right] \quad (34)$$

The power output varies with the complex stiffness, $\bar{r}(\omega)$, which depends strongly on frequency. For low-damping mechanical systems, driven well below the mechanical resonance frequency, the complex stiffness ratio is predominantly real, i.e., $\bar{r} \approx r$. Thus, the power output amplitude takes the simpler form:

$$P_{out} = \omega \frac{r}{(1 + r)^2} \left[\frac{1}{2} k_i \hat{u}_{ISA}^2 \right] \quad (35)$$

The last factor in Equation (35) is the reference mechanical energy of an active-material stack operating under dynamic conditions:

$$\hat{E}_{mechanical}^{ref} = \frac{1}{2} k_i \hat{u}_{ISA}^2 \quad (36)$$

An expression similar to Equation (36) was derived by Giurgiutiu, Rogers, and Chaudhry (1996) for an actuator operating under static conditions, but the reader's attention is drawn to the fact that the static induced strain displacement, u_{ISA} , is significantly larger than the dynamic induced strain displacement amplitude, \hat{u}_{ISA} . The difference between static and dynamic displacements may be as much as a factor of 2, which results in a 4 times difference between the

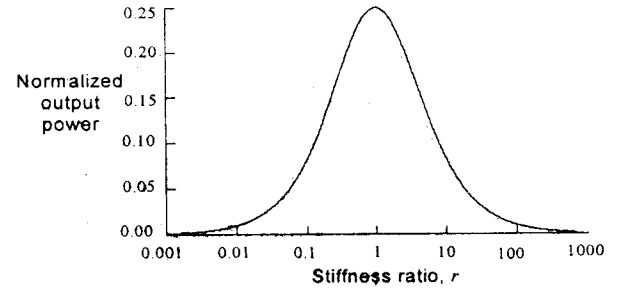


Figure 6. Variation of output power with stiffness ratio, r .

corresponding static and the dynamic reference mechanical energies.

As expected, the output power increases linearly with frequency, as shown by the first factor in Equation (35). The second factor in Equation (35) represents a modifier that accounts for the external loading conditions through the stiffness ratio, r . As the stiffness ratio increases, the output power increases at first, and then decreases (Figure 6). The maximum output power is obtained at $r = 1$, and its value is:

$$P_{out}^{max} = \omega \frac{1}{4} \left(\frac{1}{2} k_i \hat{u}_{ISA}^2 \right) \quad (37)$$

It can be seen that the maximum output power is the product between the angular frequency, ω , and 1/4 of the reference mechanical energy output. Similarly, the maximum amplitude of the output energy is given by:

$$\hat{E}_{out}^{max} = \frac{1}{4} \left(\frac{1}{2} k_i \hat{u}_{ISA}^2 \right) \quad (38)$$

The quantity \hat{E}_{out}^{max} is a frequency-independent metric that can be effectively used in comparing the dynamic performance of various active-material stacks.

Electro-Mechanical Power Conversion Efficiency of an Induced-Strain Actuator

The electro-mechanical conversion efficiency of the system consisting of the electro-active induced-strain actuator and the mechanical load can be defined as the ratio between the output mechanical power and input electrical power, i.e.,

$$\eta = \frac{|\hat{P}_{out}|}{|\hat{P}_{in}|} = \frac{\left| \omega \frac{\bar{r}(\omega)}{(1 + \bar{r}(\omega))(1 + \bar{r}(\omega))^*} \left(\frac{1}{2} k_i \hat{u}_{ISA}^2 \right) \right|}{\left| \omega \chi(v_0) \left(1 - \chi^2 \frac{\bar{r}(\omega)}{1 + \bar{r}(\omega)} \right) \frac{1}{2} CV^2 \right|} \quad (39)$$

Upon simplification,

$$\eta = \frac{\chi^2 \bar{r}(\omega)}{\chi(v_0) [1 + (1 - \chi^2) \bar{r}(\omega)] (1 + \bar{r}(\omega))^*} \quad (40)$$

The electro-mechanical conversion efficiency varies with the frequency-dependent complex stiffness, $\bar{r}(\omega)$. For low-damping mechanical systems, driven well below the mechanical resonance frequency, the complex stiffness ratio is predominantly real, i.e., $\bar{r} \approx r$. Thus, the conversion efficiency takes the simpler form:

$$\eta = \frac{\chi^2 r}{\chi(v_0)[1 + (1 - \chi^2)r](1 + r)} \quad (41)$$

As the stiffness ratio increases, the conversion efficiency, η , increases at first, and then decreases (Figure 7). The conversion efficiency has a peak at stiffness ratio values r_η , that are close to $r = 1$, but not exactly equal to 1. This optimal stiffness value, r_η , that maximizes the conversion efficiency, can be found by setting to zero the derivative of the conversion efficiency with respect to r . Hence,

$$r_\eta(\chi) = \frac{1}{\sqrt{1 - \chi^2}} \quad (42)$$

Note that the optimal stiffness ratio, r_η , varies with the electro-mechanical coupling coefficient, χ . For $\chi = 0$, the optimal stiffness ratio is $r_\eta = 1$, i.e., it coincides with the optimal stiffness ratio for maximum power output. But, for $\chi \neq 0$, the conversion efficiency is identically zero. In practice, the electro-mechanical coupling coefficient may vary between 0.6 and 0.7. Figure 8(a) shows the χ variation of the optimal stiffness ratio for maximum conversion efficiency. It can be seen that practical values of the optimal stiffness ratio, r_η , are found in the range 1.25 to 1.4. Substitution of Equation (42) into Equation (41) gives the best conversion efficiency, η_{max} , in terms of the electro-mechanical coupling coefficient, χ , and the bias voltage coefficient, v_0 , i.e.,

$$\eta_{max}(\chi, v_0) = \frac{1}{\chi(v_0)} \frac{\chi^2}{2\sqrt{1 - \chi^2} + 2 - \chi^2} \quad (43)$$

Plots of Equation (43) are given in Figure 8(b). For $v_0 = 0$

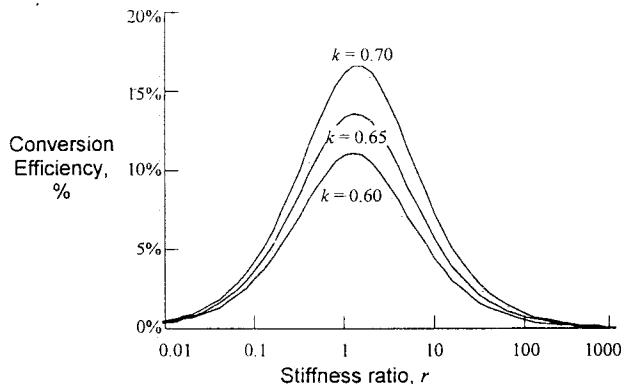


Figure 7. Variation of electromechanical power conversion efficiency with r and χ (no bias voltage, $v_0 = 0$).

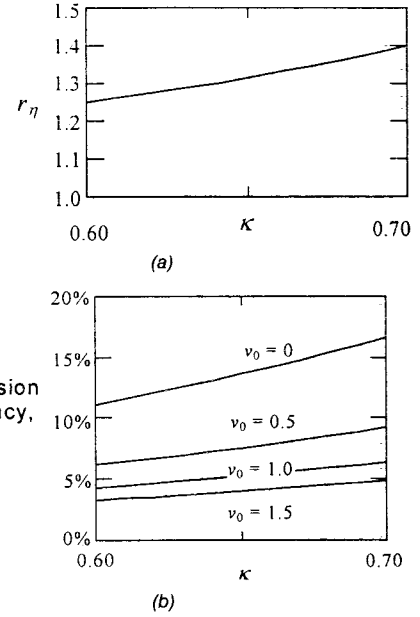


Figure 8. (a) Variation of r_η with χ and (b) variation of electro-mechanical power conversion efficiency with χ and v_0 .

(operation without bias voltage) the best conversion efficiency may vary between 11% and 17%. As bias voltage is applied, the conversion efficiency decreases. For the $v_0 = 1$ case (bias voltage equals dynamic voltage amplitude), the electro-mechanical conversion efficiency may vary between 3% and 5%.

NUMERICAL RESULTS

Data Collection and Processing

A large variety of induced-strain actuators are now available on the commercial market. In our study, we collected as much data as possible from vendor literature and by contacting directly the vendors and the manufacturers. Details about the data collection were given by Giurgiutiu, Rogers, and Chaudhry (1996). The processing of the data was performed in two stages: for static operation and for dynamic operation. The results of data processing for static operation were presented by Giurgiutiu, Rogers, and Chaudhry (1996). The results of data processing for dynamic operation are presented in this paper.

The data processing for dynamic operation (Table 1) starts with identification of the bias position, u_0 , and the dynamic displacement amplitude, \hat{u}_{ISA} . This was performed using the free expansion and free contraction strokes, u_{ISA}^+ and u_{ISA}^- , i.e.,

$$u_0 = \frac{1}{2}(u_{ISA}^+ + u_{ISA}^-), \quad \hat{u}_{ISA} = \frac{1}{2}(u_{ISA}^+ - u_{ISA}^-) \quad (44)$$

The corresponding expansion and contraction voltages, V^+

Table 1. (continued).

Identification	Bias Position u_0 (μm)	Dynamic Displacement u_{ISA} (μm)	Bias Voltage V_0 (V)	Dynamic Voltage V (V)	Apparent Electro-Mechanical Coupling Coefficient κ	Corrected Electro-Mechanical Coupling Coefficient κ'	Reactive Power Correction Factor $\chi(V_0/V)$
Polytec PI							
P-245.70	45.00	75.00	-375	-625	0.506	0.506	1.97
P-246.70	45.00	75.00	-375	-625	0.955	0.750	1.97
P-247.70	45.00	75.00	-375	-625	0.974	0.750	1.97
P-844.60	33.75	56.25	-37.5	-62.5	0.788	0.750	1.97
EDO Corp.							
E100P-2	9.00	9.00	400	400	0.919	0.750	2.62
E300P-4	33.00	33.00	400	400	0.825	0.750	2.62
E400P-3	20.00	20.00	400	400	0.974	0.750	2.62
Burleigh Instruments							
PZL-060	22.00	38.00	55	95	0.449	0.449	1.94
AVX Corp. (AVX-PMN Young's modulus was taken 91 GPa, and AVX-PZT Young's modulus was taken 70 GPa)							
AVX-PMN	8.75	8.75	75	75	0.616	0.616	2.62
AVX-PZT	4.95	8.55	55	95	0.477	0.477	1.94
TOKIN							
LA-10 \times 10 \times 1	7.50	7.50	50	50	0.890	0.750	2.62
Morgan Matroc Inc.							
70044-1	4.88	4.88	125	125	0.811	0.750	2.62
70050-1	7.51	7.51	125	125	0.636	0.636	2.62
70051-1	7.51	7.51	125	125	0.763	0.750	2.62

and V^- , were used to calculate the bias voltage, V_0 , and the dynamic voltage amplitude, V , i.e.,

$$V_0 = \frac{1}{2}(V^+ + V^-), \quad V = \frac{1}{2}(V^+ - V^-) \quad (45)$$

Hence, the bias voltage coefficient, $v_0 = V_0/V$, and the reactive power correction factor, $\chi(v_0) = 1 + 1.62v_0$ were computed. The apparent electro-mechanical coupling coefficient, $\kappa = k_i \hat{u}_{ISA}^2 / CV^2$, was calculated using Equation (11). By limiting its upper value to 0.75, we obtained the corrected electro-mechanical coupling coefficient, κ' .

The output energy and energy densities were calculated next (Table 2). The maximum output energy amplitude (stiffness match, $r = 1$) was calculated with Equation (38), i.e., $\hat{E}_{out}^{max} = (1/4)[(1/2)k_i \hat{u}_{ISA}^2]$. By dividing the maximum output energy amplitude, \hat{E}_{out}^{max} , by the active-material volume and mass, the volume and mass energy densities of the actuators for dynamic operation were obtained. Note that these dynamic-operation energy densities are substantially lower than the static-operation energy densities presented in Giurgiutiu, Rogers, and Chaudhry (1996). The main difference between static and dynamic energy values stems from the fact that, due to the asymmetric operation of the induced-strain actuator, the dynamic displacement amplitude is significantly lower than the static displacement (in many cases, a factor of 1/2 is applied to the displacement values, resulting in a factor of 1/4 on the energy values). Finally, Equation (45) was used to calculate the best energy

conversion efficiency. The stiffness ratio value, r_η , at which the best conversion efficiency takes place, was calculated using Equation (44).

Discussion of Results

Figure 9 presents a number of charts comparing the performance of the electro-active induced-strain actuators considered in this study. The apparent electro-mechanical coupling coefficient, κ , can serve as a first indicator of the actuator performance. The variation of the apparent electro-mechanical coupling coefficient is shown in Figure 9(a). Values as low as 0.45 are observed in some cases, but the majority of the commercially-available induced-strain actuators seem to claim a very good electro-mechanical coupling performance.

A comparison of the maximum dynamic energy output that can be extracted from the commercially-available induced-strain actuators is given in Figure 9(b). It seems that, at present, only one company, Polytec PI, Inc., has off-the-shelf induced-strain actuator products with large dynamic energy output capabilities (0.260 J peak for P-247.70). However, similar high-output energy products may also be available from other manufacturers, by special order. Figure 9(c) compares the energy density per unit volume, which is found to vary from 0.7 to 3.7 J/dm³. For many induced-strain actuators, a mid-range value of around 2 J/dm³ seems to be common. The high end values, around 3.7 J/dm³, are reached by the Polytec PI and AVX products. Figure 9(d) compares the energy density per unit mass,

which varies from 0.091 to 0.482 J/kg. For many induced-strain actuators, a mid-range value of around 0.2 J/kg seems to be common. The high-end value of 0.482 J/kg is reached only by one Polytec PI product (P-247.70). Figure 9(e) gives an energy density comparison based on energy per unit cost in mJ/\$1000. Examination of this chart indicates that some companies are capable of marketing products with specific energy costs remarkably lower than others. This observation does not seem to be influenced by the processing method, since it affects adhesively-bonded and co-fired products equally.

Figure 9(f) presents a comparison of the best energy conversion efficiencies that can be expected from these induced-strain actuators under the most favorable stiffness ratio conditions. As described by Equation (41), this coefficient represents the ratio between the output mechanical energy and the input electrical energy. These energies are predominantly reactive (capacitance in the electrical energy, and spring in the mechanical energy), and hence the efficiency coefficient is defined as the ratio between their peak values. Note that the peak value per cycle of the reactive electrical energy is strongly influenced by the presence of the bias voltage, as described by Equation (29). The energy conversion efficiency is also influenced by the electro-mechanical coupling coefficient, κ , as shown in Equation (43). The energy conversion efficiency results [Figure 9(f)], indicate that the energy conversion efficiency seems to vary

from 2.90% to 10.33%, with the high-end products also having high values of conversion efficiency.

CONCLUSIONS

The dynamic power and energy capabilities of commercially-available induced-strain actuators operating against an external mechanical load have been considered. The mechanical load was modeled by a spring-mass-damping system of equivalent dynamic stiffness ratio, $\bar{F}(\omega)$. In the beginning of the study, clarification of some fundamental concepts regarding the active and reactive components of power and energy specific to the dynamic operation of electro-active induced-strain actuators was done. It was found that for lightly-damped systems, the reactive power and energy are dominant, and this aspect was found to be fundamentally different from the conventional analysis of electric motors and other traditional electro-mechanical devices.

A number of specific concepts were introduced and/or clarified in the present study. This *apparent electro-mechanical coupling coefficient*, κ , of an electro-active induced-strain actuator was introduced by Equation (11) via a secant-method linearization procedure. The *reactive power amplification coefficient*, $\chi(v_0)$, was defined through Equation (27) in terms of the complex power magnitude,

Table 2. Dynamic energy, energy densities, and best conversion efficiency values for 14 commercially-available induced-strain actuators.

Identification	Active Material Type	Price (\$)	Maximum Dynamic Energy Output E_{out} (J)	Best Energy Conversion Efficiency η (%)	Best Stiffness Ratio for Energy Conversion r_r	Active Material Volume V_{ISA} (mm^3)	Active Material Mass m_{ISA} (g)	Output Energy per	Output	Output
								Active Material Volume E_e/V_{ISA} (J/dm^3)	Energy per Active Material Mass E_e/m_{ISA} (J/kg)	Energy per Unit Cost E_e/Price (mJ/\$1000)
Polytec PI										
P-245.70	HVPZT	2250	0.0056	3.74%	1.16	7929	61.8	0.709	0.091	2.5
P-246.70	HVPZT	4940	0.1336	10.33%	1.51	49063	382.7	2.723	0.349	27.0
P-247.70	HVPZT	7790	0.2602	10.33%	1.51	69163	539.5	3.761	0.482	33.4
P-844.60	LVPZT	4565	0.0131	10.33%	1.51	10990	85.7	1.188	0.152	2.9
EDO Corp.										
E100P-2	PMN	315	0.0010	7.78%	1.51	703	5.5	1.440	0.183	3.2
E300P-4	PMN	710	0.0218	7.78%	1.51	13036	102.3	1.671	0.213	30.7
E400P-3	PMN	480	0.0110	7.78%	1.51	6924	54.4	1.589	0.202	22.9
Burleigh Instruments										
PZL-060	PZT	1090	0.0007	2.90%	1.12	960	7.5	0.733	0.093	0.6
AVX Corp.										
AVX-PMN	PMN	125	0.0012	4.54%	1.27	404	4.4	2.975	0.273	9.6
AVX-PZT	PZT	125	0.0012	3.32%	1.14	395	4.6	2.922	0.251	9.2
TOKIN										
LA-10 × 10 × 1	PZT	227	0.0016	7.78%	1.51	1656	13.2	0.972	0.122	7.1
Morgan Matroc Inc.										
70044-1	PZT-5H	231	0.0032	7.78%	1.51	2250	16.9	1.426	0.190	13.9
70050-1	PZT-5H	316	0.0090	4.92%	1.30	6000	45.0	1.502	0.200	28.5
70051-1	PZT-5H	367	0.0141	7.78%	1.51	9375	70.3	1.502	0.200	38.4

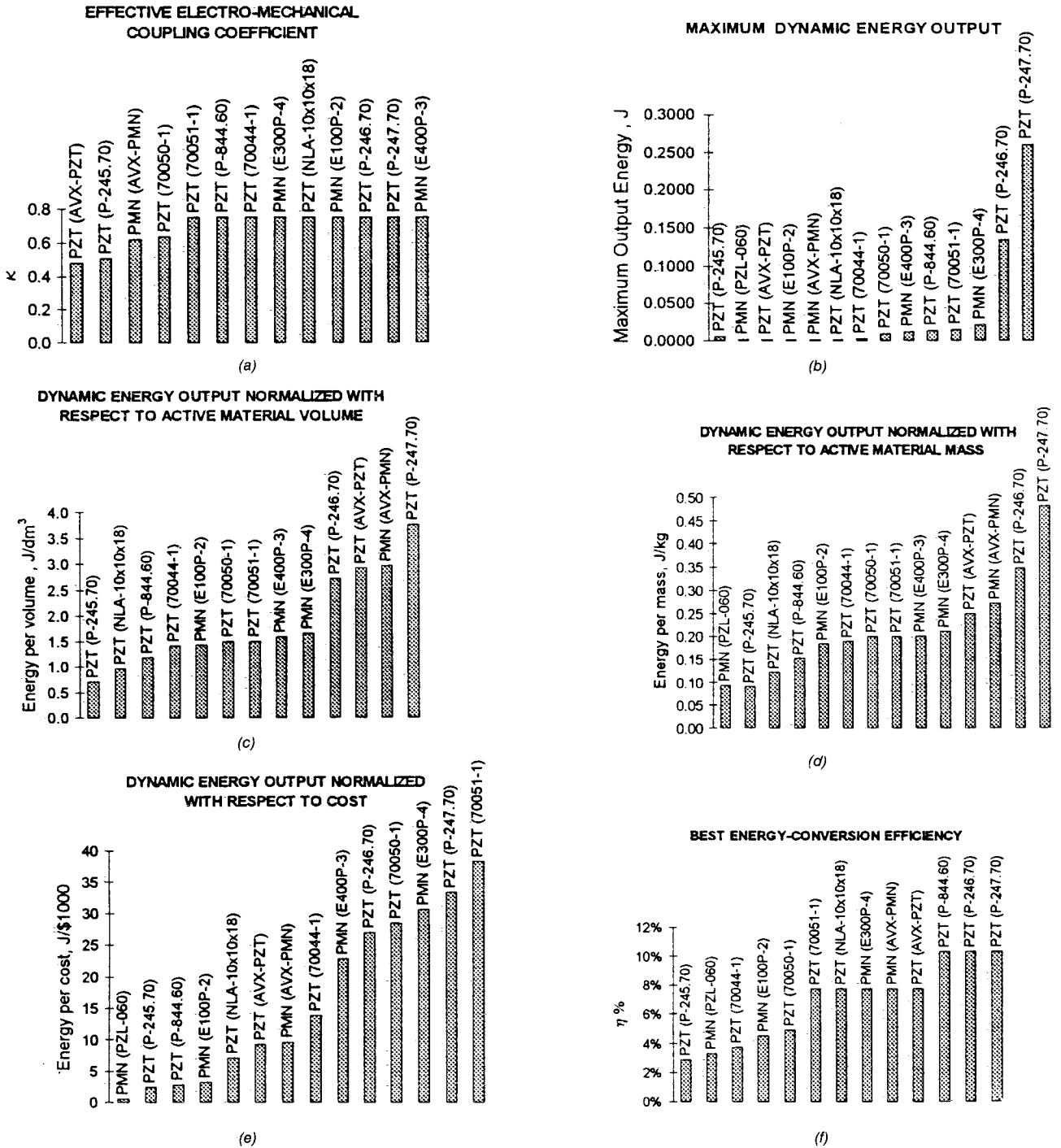


Figure 9. Charts of predicted behavior under dynamic operation calculated using vendor data for 14 commercially-available induced-strain actuators.

$|\bar{P}| = |\bar{Y}| V^2$, and the *bias-voltage coefficient*, $v_0 = V_0/V$. A linearized expression for the reactive power amplification coefficient, $\chi(v_0)$, was given in Equation (28) for the range $-1.5 < v_0 < 1.5$. Hence, the reactive input power requirements for an electro-active induced-strain actuator were expressed by Equation (31) in terms of the reference electrical energy, $(1/2)CV^2$, the reactive power

amplification coefficient, $\chi(v_0)$, the apparent electro-mechanical coupling coefficient, κ , and the stiffness ratio, r .

The output power and energy were expressed in terms of the reference mechanical energy, $(1/2)k_i u_{ISA}^2$, and an extraction factor that depends on the stiffness ratio and has its maximum value equal to 1/4. Hence, the maximum output energy was identified as $\dot{E}_{out}^{max} = (1/4)[(1/2)k_i u_{ISA}^2]$, while

the corresponding output power was found to be, simply, $\dot{P}_{out}^{max} = \omega \dot{E}_{out}^{max}$. Finally, the ratio between the output and input power was used to define the electro-mechanical conversion efficiency, η , of the electro-active induced-strain actuator operating the mechanical load. The maximum possible value, η_{max} , of the electro-mechanical conversion efficiency was calculated in terms of ν_0 and κ and given as a simple formula in Equation (43). Remarkably, the stiffness ratio value at which the best conversion efficiency is attained does not coincide with the stiffness match value at which maximum energy output is obtained. However, the difference between the two optimal stiffness ratios (for best energy conversion and for maximum energy output) was not found to be very large.

The study is accompanied by extensive numerical data, shown in tables and charts. It was found that maximum dynamic output energy of commercially-available electro-active induced-strain actuators can be as high as 0.260 J. The corresponding energy density values per unit volume and unit mass were found in the range 0.7–3.7 J/dm³, and 0.091–0.482 J/kg, respectively. Not surprisingly, these values are lower than those for static operation (Giurgiutiu, Rogers, and Chaudhry, 1996) since, due to the asymmetric behavior of the induced-strain actuators, the dynamic displacement amplitude, \hat{u}_{ISA} , is much lower (typically 1/2) than the static stroke, u_{ISA} . Electro-mechanical energy conversion efficiency was found to be in the range 2.9% to 10.3%, while the optimal stiffness ratio for best energy conversion was found in the range 1.12 to 1.51.

The present study offers useful dynamic performance data that can be directly incorporated in the design of mechanical and hydraulic devices utilizing off-the-shelf induced-strain actuators. The present study and the previous static-operation study by Giurgiutiu, Rogers, and Chaudhry (1996) form a valuable guide for practicing engineers penetrating the active-materials design area. The linearization procedure used in this study to model the full-stroke dynamic behavior ensures that all the important parameters (input power, output power, conversion efficiency, and electro-mechanical coupling coefficient) are expressed in terms of standard vendor information and do not require insight into the intimate behavior of the active material used inside the induced-strain actuator. For these reasons, the analysis is general and can be readily applied to other similar products.

It can also lead directly to formulation of industry standards that will greatly facilitate the development, use, and marketing of this novel class of actuators.

ACKNOWLEDGEMENTS

The authors gratefully acknowledge the support of the U.S. Army Research Office—University Research Initiative Program, Grant No. DAAL03-92-0181, Dr. Gary Anderson, Program Manager. The authors would also like to thank all the contact persons in the companies participating in the survey, and especially: Candace Borque from Polytec PI Inc.; Gordon Cook from EDO Corporation, Electro-Acoustic Division; Mel Goodfriend from ETREMA Products, Inc.; Andy Ritter from AVX Corporation, Research Laboratory; and Mike Konno from Tokin America, Inc., who extended their help, guidance and constructive intellectual interaction in clarifying some of the more subtle points encountered during the survey.

REFERENCES

- Anon. 1988. "IEEE Standard on Piezoelectricity", ANSI/IEEE Std 176-1987, Institute of Electrical and Electronics Engineers, Inc., New York.
- AVX Corporation. 1995. Product Catalogues and Private Communications, Myrtle Beach, SC 29577.
- Burleigh Instruments, Inc. 1995. Product Catalogues and Private Communications, Burleigh Park, Fishers, NY 14453.
- EDO Corporation. 1996. Product Catalogues and Private Communications, 2645 South 300 West, Salt Lake City, Utah 84115.
- Giurgiutiu, V., Z. Chaudhry and C. A. Rogers. 1994. "The Analysis of Power Delivery Capabilities of Induced-Strain Actuators for Dynamic Applications", June 5–8, Colonial Williamsburg, VA, Technomic Pub. Co., Inc., pp. 565–576.
- Giurgiutiu, V., C. A. Rogers and Z. Chaudhry. 1996. "Energy-Based Comparison of Solid-State Induced-Strain Actuators", *Journal of Intelligent Material Systems and Structures*, 7(1):4–14.
- Kinetic Ceramics, Inc. 1995. Product Catalogues and Private Communications, 26242 Industrial Blvd., Hayward, CA 94545.
- Morgan Matroc. 1995. Electroceramics Division, Product Catalogues and Private Communications, 232 Forbes Rd., Bedford, Ohio 44146.
- Polytec PI, Inc. 1995. Product Catalogues and Private Communications, 3001 Redhill Ave., Bldg. 5-102, Costa Mesa, CA 92626.
- Tokin America, Inc. 1995. Product Catalogues and Private Communications, 155 Nicholson Ln., San Jose, CA 95134.